Global entanglement in ground state of $\{Cu_3\}$ single-molecular magnet with magnetic field*

Li Ji-Qiang (李纪强) and Zhou Bin(周 斌)†

Department of Physics, Hubei University, Wuhan 430062, *China*

(Received 19 February 2014; revised manuscript received 21 March 2014; published online 22 May 2014)

We investigate global entanglement in the ground state of single-molecular magnet $Na_9[Cu_3Na_3(H_2O)_9(\alpha\text{-}AsW_9O_{33})_2]\cdot 26H_2O$ with an external magnetic field. The concurrence, tangle, and measure function Q, which characterize the pairwise entanglement, 3-party entanglement and total entanglement, respectively, are calculated numerically at zero temperature. The results show that the magnitude and direction of the applied magnetic field play a significant role in the properties of three kinds of entanglement measures. We give a physical interpretation of the variation of the global entanglement with the magnetic field. Finally, the phase diagram of the global entanglement characterized by the critical magnetic fields is presented.

Keywords: global entanglement, single-molecular magnet, triangular spin ring

PACS: 03.65.Ud, 03.67.Mn, 75.10.Jm, 75.50.Xx **DOI:** 10.1088/1674-1056/23/7/070302

1. Introduction

Entanglement is a fundamental feature of the quantum mechanics. In recent years, entanglement has been regarded as a potential valuable resource for quantum information and quantum computing processing, which has attracted much attention from both theoretical and experimental aspects. The 3-qubit entanglement states have shown their superiority over the 2-qubit states in quantum teleportation,[1] dense coding[2] and quantum cloning.[3] There are different inequivalent entanglement classes not only under deterministic local operations and classical communication, but even under their stochastic analog.[4,5] Many criteria have been proposed to distinguish separable from entangled pure states for the 3-qubit system. Coffman *et al.*[6] introduced the concept of the residual entanglement to represent the genuine 3-party entanglement derived from an inequality. Meyer *et al.*[7] firstly defined a polynomial measure that not only can be applied to tripartite but also to multipartite entanglement consisting of spin-1/2 particles. Later Brennen[8] rewrote the polynomial measure in another form which characterizes the total of contributions from various kinds of entanglement. Rungta *et al.*[9] proposed the so-called *i*-concurrence that exhibits the entanglement property between the subsystem of *i*-th qubit and other qubits. Up to now, the properties of quantum entanglement in different qubit systems have been investigated extensively.[10–19]

It is significant to find a kind of practical material for the implementation of quantum information and quantum computing. Nanoscale molecular magnets have attracted considerable attention due to their novel quantum effects.[20–26] Furthermore, single-molecular magnets are viewed as a promising candidate for realizing encoding and manipulation of quantum information.[27–32] Among the different families of single-molecular magnets, $Na_9[Cu_3Na_3(H_2O)_9(\alpha\text{-}AsW_9O_{33})_2]\cdot 26H_2O$ (hereafter abbreviated as $\{Cu_3\}$) has also attracted much research interest recently. $\{Cu_3\}$ has a sandwich-type structure with D_{3h} symmetry.[33] The central belt, separated by two $[\alpha\text{-}AsW_9O_{33})_2]^{9-}$ subunits, consists of three $CuO_4(H_2O)$ square pyramids linked by Na^+ ions.[23] In the unit cell, there are two triangular rings of Cu^{2+} ions. Static susceptibility suggests that Cu^{2+} ions are antiferromagnetically coupled.[22] Choi *et al.*[23] observed the half step magnetization in $\{Cu_3\}$. Stowe *et al.*[24] reported its high-frequency electron paramagnetic resonance spectroscopy. Moreover, it is a perfect material performing as a quantum logical gate for its effective two-level behavior.[34] $\{Cu_3\}$ can be viewed as a triangular spin-1/2 ring (i.e., a 3-qubit system) in which every Cu^{2+} ion is equivalent to a qubit. The structure of the $\{Cu_3\}$-type triangular spin ring is actually an isosceles triangle. The distances between the neighbor Cu^{2+} ions are $d_{12} = 4.689$ Å and $d_{23} = d_{13} = 4.696$ Å, respectively.[23] Hou *et al.*[35] studied the thermal entanglement in a $\{Cu_3\}$-type molecular spin ring, however, the molecule was merely considered as an ideal model. Recently, Li *et al.*[36] investigated the pairwise thermal entanglement in $\{Cu_3\}$ with an external magnetic field by using the realistic material parameters. On the other hand, further research of the global entanglement in $\{Cu_3\}$ at zero temperature is required.

*Project supported by the National Natural Science Foundation of China (Grant No. 11274102), the Program for New Century Excellent Talents in Universities, China (Grant No. NCET-11-0960), and the Specialized Research Fund for the Doctoral Program of Higher Education of China (Grant No. 20134208110001).

†Corresponding author. E-mail: binzhou@hubu.edu.cn

© 2014 Chinese Physical Society and IOP Publishing Ltd

In this paper, we will give a theoretical analysis on the properties of global entanglement in the ground state of $\{Cu_3\}$ with an external magnetic field. The concurrence, tangle, and measure function Q, which characterize the pairwise entanglement, 3-party entanglement and total entanglement, respectively, are calculated numerically at zero temperature when the magnetic field is applied in different directions. We also present the phase diagram of global entanglement characterized by the critical magnetic fields.

2. Model and method

The effective spin Hamiltonian of $\{Cu_3\}$-type triangular spin ring with external magnetic field can be written as follows:[23]

$$\mathcal{H} = \sum_{l=1}^{3}\sum_{\alpha=x,y,z} J_{ll+1}^{\alpha}\boldsymbol{S}_l\cdot\boldsymbol{S}_{l+1} + \sum_{l=1}^{3}\boldsymbol{D}_{ll+1}\cdot[\boldsymbol{S}_l\times\boldsymbol{S}_{l+1}] + \mu_{\rm B}\sum_{l=1}^{3}\boldsymbol{S}_l\cdot\tilde{\boldsymbol{g}}_{ll+1}\cdot\boldsymbol{H}_l, \quad (1)$$

with the exchange coupling constant J, the magnetic field vector $\boldsymbol{H}$, the spin operator $\boldsymbol{S}$, the Bohr magnetron $\mu_{\rm B}$, the Landé g-factor tensor $\tilde{\boldsymbol{g}}$ and the Dzyaloshinkii–Moriya (DM) vector $\boldsymbol{D}$. Choi *et al.*[23] reported the fitting values for all the parameters of the effective spin Hamiltonian (1) through an electronic spin resonance (ESR) experiment, magnetization measurements and symmetry analysis of the system, J is given by the magnetization measurement, $J_{12}^{x,y} = 4.50$ K, $J_{12}^{z} = 4.56$ K, $J_{23}^{x,y} = J_{31}^{x,y} = 4.03$ K and $J_{23}^{z} = J_{31}^{z} = 4.06$ K, $\widetilde{g}$ is determined by the ESR experiment, $g_{11}^{x,y} = 2.25$, $g_{22}^{x,y} = 2.10$, $g_{33}^{x,y} = 2.40$, and $g_{ii}^{z} = 2.06$ $(i = 1,2,3)$. A fitting to the angular dependence of the resonance fields demonstrates $D_{12}^{x,y} = D_{ii+1}^{z} = 0.53$ K $(i = 1,2,3)$. The in-plane component of the DM vectors obeys approximately C_3 symmetry:[23] $(D_{23}^{x}, D_{23}^{y}) = \mathcal{R}(2\pi/3)\times(D_{12}^{x}, D_{12}^{y})$ and $(D_{31}^{x}, D_{31}^{y}) = \mathcal{R}(4\pi/3)\times(D_{12}^{x}, D_{12}^{y})$, where $\mathcal{R}(\theta)$ denotes a rotation of the triangle by θ.

The measure function Q for the pure state of a multipartite was firstly put forward by Meyer and Wallach,[7] and was later presented in the following form by Brennen[8]

$$Q(|\psi\rangle) = \frac{1}{N}\sum_{i=1}^{N} IC_i^2, \quad (2)$$

where IC_i is the so-called i-concurrence that is related to the reduced density matrix ρ_i for the subsystem i. The i-concurrence is given by[9]

$$IC_i = \sqrt{2[1-{\rm Tr}(\rho_i^2)]}. \quad (3)$$

For the special case of a 3-qubit system, Coffman *et al.*[6] introduced the tangle, also called the residual entanglement. The tangle is defined as

$$\begin{aligned}\tau &= IC_1^2 - C_{12}^2 - C_{13}^2 = IC_2^2 - C_{12}^2 - C_{23}^2 \\ &= IC_3^2 - C_{13}^2 - C_{23}^2, \end{aligned} \quad (4)$$

where C_{ij} is the concurrence of the i-th and j-th qubits and can be denoted by[37,38]

$$C_{ij} = \max\{\lambda_1 - \lambda_2 - \lambda_3 - \lambda_4, 0\}, \quad (5)$$

where $\{\lambda_1, \lambda_2, \lambda_3, \lambda_4\}$ are the square roots of the eigenvalues of operator R_{ij} arranged in descending order, and the operator R_{ij} can be written as

$$R_{ij} = \rho_{ij}(\sigma_i^y \otimes \sigma_j^y)\rho_{ij}^*(\sigma_i^y \otimes \sigma_j^y), \quad (6)$$

where ρ_{ij} is the reduced density matrix of the pair comprising of i-th and j-th qubits, and σ_i^y refers to the y-component of the Pauli matrix. It is seen that Q is the sum of squared concurrences plus tangle for tripartite

$$Q = \frac{2}{3}(C_{12}^2 + C_{23}^2 + C_{13}^2) + \tau. \quad (7)$$

The total entanglement measured by Q consists of different entanglement contributions, i.e., the pairwise entanglement measured by the concurrence and the 3-party entanglement measured by the tangle.[39] Noted that each measure emphasizes a specific feature of entanglement in a many-body system.

3. Results and discussion

In principle, the problem of 3-qubit spin models can be solved analytically. However, due to the anisotropy of the magnetic parameters of the $\{Cu_3\}$-type triangular spin ring considered in this paper, the analytical expressions of eigenfunctions and the corresponding eigenvalues of the effective spin Hamiltonian (1) are too complex to be compactly given. Thus in order to obtain explicit physical results, we resort to a numerical calculation method based on the material parameters of the $\{Cu_3\}$ single-molecular magnet given above. First, we obtain the eigenvalues and eigenfunctions of the $\{Cu_3\}$-type triangular spin ring by numerical diagonalization of Hamiltonian (1). Then, according to the standard process given in the references to calculate numerically the concurrence C_{ij}, the tangle τ and the measure function Q at zero temperature when the magnetic field is applied in different directions. Energy level diagrams of the Hamiltonian (1) are shown in Fig. 1. At zero field, the upper four levels refer to $S^{\rm T} = 3/2$ states and the lower four refer to $S^{\rm T} = 1/2$ states.[23] We consider the ground state of the system. The eigenenergy of the ground state is presented as E_0 in Fig. 1, and the corresponding eigenfunction is written as $|\psi_0\rangle = \sum_{q_i\in\{0,1\}} \alpha_{q_1q_2q_3}|q_1q_2q_3\rangle$.

The case that an applied magnetic field is along the Z axis (i.e., $H \perp$ the plane comprising the three copper ions)

is considered first. The dependence of C_{ij}, τ, and Q in the ground state of $\{Cu_3\}$ on the magnetic field H_z are plotted in Fig. 2. When the magnetic field is absent, $C_{12} = 0.813$, $C_{23} = C_{13} = 0.543$, $\tau = 0$, and $Q = 0.834$, respectively. Numerical results show that when $|H_z|$ is changed from zero, C_{ij} and Q are almost unchanged, that is, an approximate plateau occurs at the low field. With increasing the magnitude of magnetic field H_z, they monotonically decrease to zero. Moreover, C_{23} and C_{13} are strictly equal. Actually, the exchange coupling constants between site 2 and site 3 have the same values as those between site 1 and site 3 due to the isosceles-triangle structure of the spin ring. Interestingly, it is noted that the 3-party entanglement measured by τ vanishes. Thus, in this case only the pairwise entanglement contributes to the total entanglement.

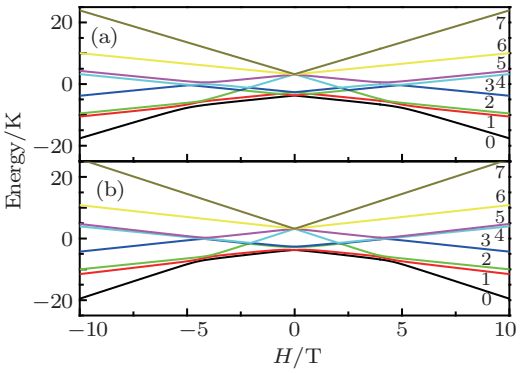


Fig. 1. (color online) The dependence of energy levels for the Hamiltonian (1) on an applied magnetic field. (a) The applied magnetic field along the Z axis (i.e., perpendicular to the plane comprising the three copper ions); (b) the applied magnetic field along the X axis (i.e., parallel to the plane).

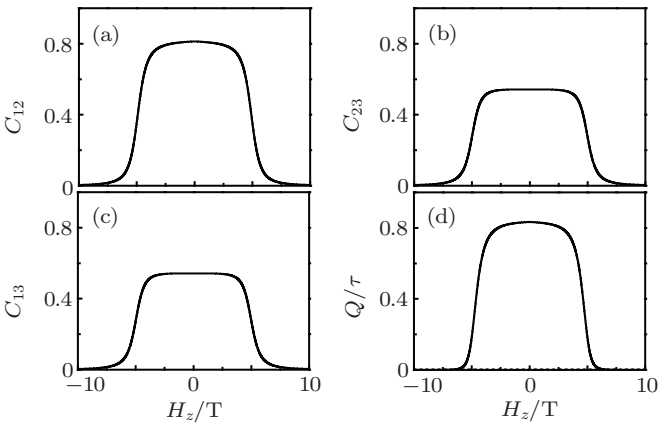


Fig. 2. C_{ij}, τ and Q in the ground state of $\{Cu_3\}$ versus the magnetic field along the Z axis. (a) C_{12}; (b) C_{23}; (c) C_{13}; (d) Q (the solid line) and τ (vanishes).

The properties of entanglement mentioned above originate from the configuration of the energy levels and the corresponding states. When $|H_z|$ is smaller than about 4 T, the ground state is the lowest $S^{\mathrm{T}} = 1/2$ state of which all the measures remain unchanged nearly. The gradual decreasing of measures arises from a tiny admixture of level 1 to level 0 in the field interval of approximately 4–5.3 T. Furthermore, from Fig. 1, it is shown that the ground state transits from the lowest $S^{\mathrm{T}} = 1/2$ state to the lowest $S^{\mathrm{T}} = 3/2$ one with increasing the magnetic field.[23] To gain more insight, we calculate the modular square of expansion coefficients with respect to the standard basis in the ground state numerically, shown in Fig. 3. Our calculation demonstrates that the ground state is doublet at zero field and the two degenerate states have the same values of entanglement measures. One of the doublets consists of $\{|100\rangle, |010\rangle, |001\rangle\}$, while the other consists of $\{|110\rangle, |101\rangle, |011\rangle\}$ instead.

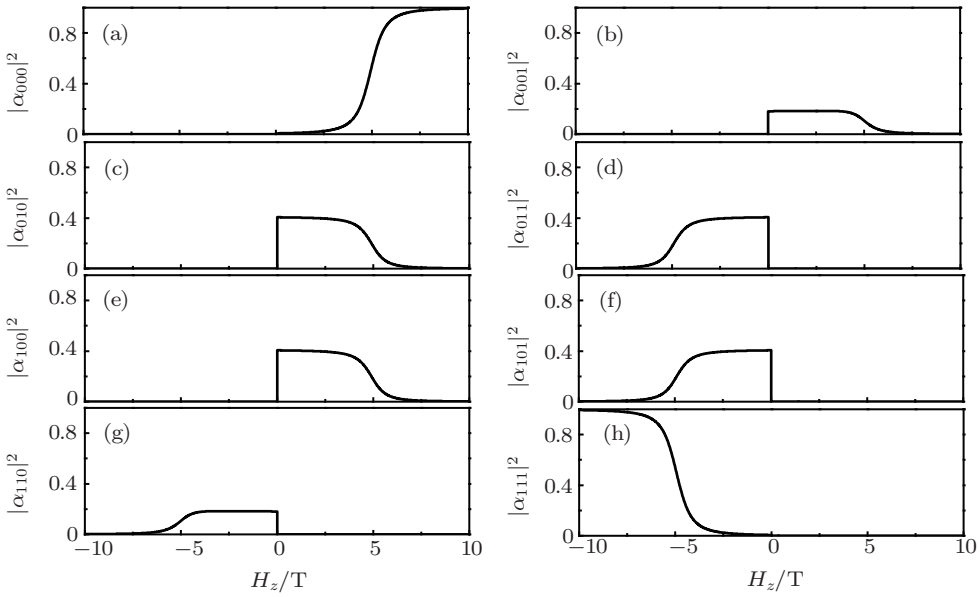


Fig. 3. The modular square of the expansion coefficients with respect to the standard basis in the ground state versus the applied magnetic field along the Z axis: (a) $|\alpha_{000}|^2$, (b) $|\alpha_{001}|^2$, (c) $|\alpha_{010}|^2$, (d) $|\alpha_{011}|^2$, (e) $|\alpha_{100}|^2$, (f) $|\alpha_{101}|^2$, (g) $|\alpha_{110}|^2$, (h) $|\alpha_{111}|^2$.

When a positive low field is applied, the ground state is mainly made up of three standard bases, i.e., $|100\rangle$, $|010\rangle$, and $|001\rangle$, which is similar to the generalized W state $|W\rangle = \alpha|100\rangle + \beta|010\rangle + \gamma|001\rangle$ that contains no genuine 3-party entanglement measured by τ.[6,39] Under this circumstance, Q can be described by the sum of the squared concurrences [see Eq. (7)]. However, the standard basis $|000\rangle$ has an admixture into the ground state with increasing the magnetic field. Furthermore, when the stronger field is applied, the ground state just consists of the standard basis $|000\rangle$ which is proved to be a separable state, thus all the values of entanglement measures vanish. Similarly, when a negative field is applied, the components of the ground state turn to $|110\rangle$, $|101\rangle$, and $|011\rangle$, which is similar to the generalized W state $|W\rangle = \alpha|011\rangle + \beta|101\rangle + \gamma|110\rangle$, then the ground state becomes $|111\rangle$ with a stronger field.

The characteristics of entanglement with the applied magnetic field parallel to the plane of $\{Cu_3\}$-type triangular spin ring are essentially different from the case of the applied magnetic field perpendicular to the plane discussed above. Shown in Fig. 4 are measures versus the magnetic field along the X axis. It is noted that all the measures undergo a sudden change at zero field. Thus, the in-plane magnetic field can induce the quantum phase transition near zero field. Compared with C_{23} and C_{13}, C_{12} shows an entirely different variation tendency. When the magnetic field along the X axis is applied, C_{12} firstly reduces sharply to 0.637 from 0.813 at zero field. With increasing the magnetic field it increases to a maximum 0.958 at the field of 2.051 T, and then decreases. On the other hand, C_{23} and C_{13} exhibit a more complex behavior. When $|H_x|$ is changed from zero, they decrease firstly both from 0.195 until arriving at a local minimum, 0.101 and 0.042 at the magnetic field of 0.963 T and 0.885 T, respectively. Then they increase again and stop to reduce gradually to zero after arriving at another local maximum. It is noted that the magnetic field along the X axis can induce a nonzero 3-party entanglement measured by τ. When the magnetic field along the X axis is applied, τ firstly skips sharply to 0.261 from 0 at zero field. Then τ monotonously decreases to zero with increasing the magnetic field. On the other hand, Q reduces sharply from 0.834 at zero field to 0.582 when the magnetic field along the X axis is applied. With increasing the magnetic field, it increases to a maximum 0.648 at the field of 1.681 T, and then decreases to zero.

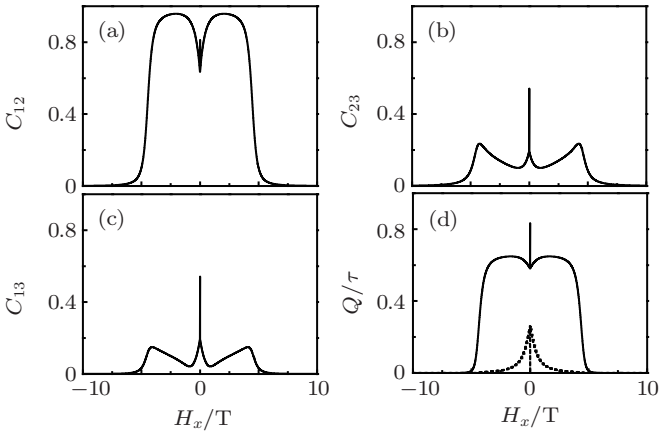


Fig. 4. C_{ij}, τ and Q in the ground state of $\{Cu_3\}$ versus the magnetic field along the X axis. (a) C_{12}; (b) C_{23}; (c) C_{13}; (d) Q (the solid line) and τ (the dashed line).

We also numerically calculate the modular square of expansion coefficients with respect to the standard basis in ground state when the magnetic field along the X axis is applied. The results are shown in Fig. 5. In fact, at a low magnetic field, the ground state exists as $\alpha_{001}|001\rangle + \alpha_{010}|010\rangle + \alpha_{011}|011\rangle + \alpha_{100}|100\rangle + \alpha_{101}|101\rangle + \alpha_{110}|110\rangle$. While $|H_x|$ is large enough, the ground state becomes $(|0\rangle \pm |1\rangle)^{\otimes 3}/\sqrt{2^3}$, thus all the values of entanglement measures vanish.

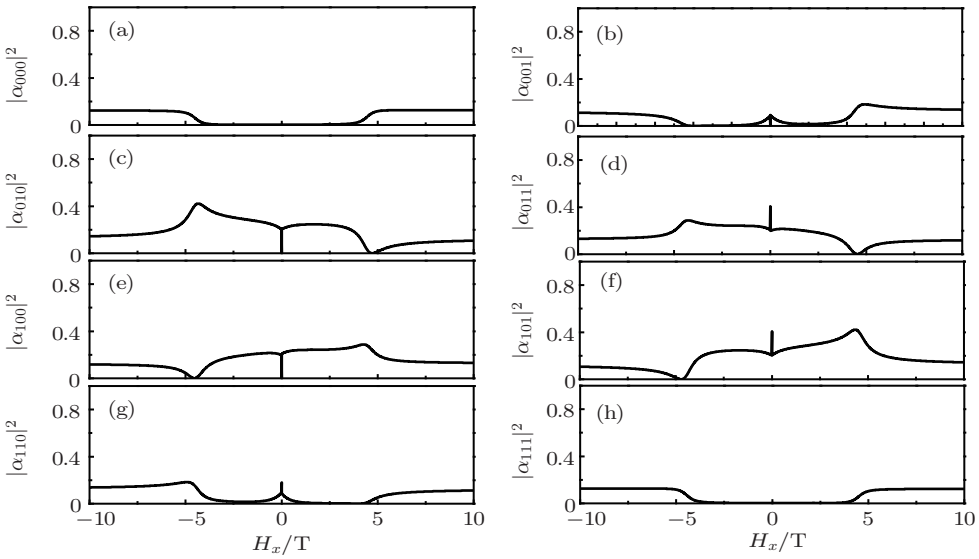


Fig. 5. The modular square of coefficients of the standard basis constituting the ground state versus the applied magnetic field along the X axis: (a) $|\alpha_{000}|^2$, (b) $|\alpha_{001}|^2$, (c) $|\alpha_{010}|^2$, (d) $|\alpha_{011}|^2$, (e) $|\alpha_{100}|^2$, (f) $|\alpha_{101}|^2$, (g) $|\alpha_{110}|^2$, (h) $|\alpha_{111}|^2$.

In Fig. 6, we plot the dependence of C_{ij}, τ, and Q on the applied magnetic field along the Y axis. The sudden changes of all the measures at zero field also occur like the case of the field along the X axis. The variation tendency of C_{12} versus the field along the Y axis is similar to the case that along the X axis, as well as τ and Q. This results from the special symmetry of the triangular spin ring. It is noted that x components and y components of the exchange coupling constant J are the same, as well as the Landé g-factor tensor $\tilde{\boldsymbol{g}}$. A slight oscillation occurs when C_{23} and C_{13} vary with the field along the Y axis, which is consistent with the thermal entanglement at very low temperature.[36] The differences in variation tendency mainly arise from the differences in components of the DM vector $\boldsymbol{D}$. Remarkably, this kind of difference affects the concurrence for a specific pair of qubits when the direction of the in-plane magnetic field changes. Nevertheless, numerical results show that values of τ for the two cases with the field along the Y axis and along the X axis are in excellent agreement. Furthermore, the behavior of Q in the case with the field along the Y axis is qualitatively similar to the case with the field along the X axis, in fact only for a small range of magnetic field (2.1 T $\leq H \leq$ 4.2 T) a little variance (smaller than 0.05) occurs.

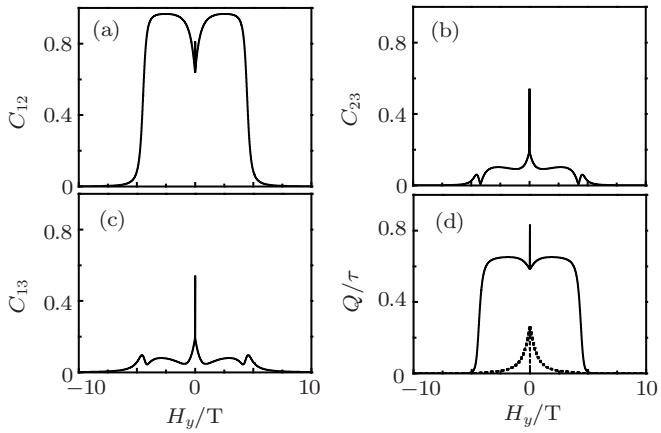


Fig. 6. C_{ij}, τ, and Q in the ground state of $\{Cu_3\}$ versus the magnetic field along the Y axis. (a) C_{12}; (b) C_{23}; (c) C_{13}; (d) Q (the solid line) and τ (the dashed line).

The phase diagram of the global entanglement characterized by the critical magnetic fields is plotted in Fig. 7. Only in the area surrounded by the critical curve does the global entanglement exist (we take the values smaller than 10^{-3} for zero here). It is obvious that the nonzero regime of Q is larger than that of τ. When the magnetic field is beyond a certain critical value, the entanglement vanishes. For instance, when $|H_z|$ maintains larger than 4.21 T, one cannot gain the 3-party entanglement by applying the magnetic field along the X axis.

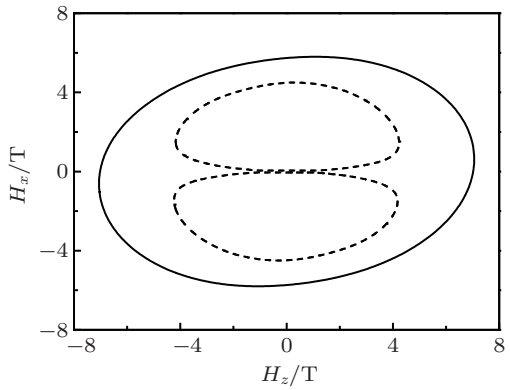


Fig. 7. Phase diagrams of Q and τ in the ground state of $\{Cu_3\}$ when the magnetic field consists of an x component and a z component. The solid line represents Q and the dashed line represents τ (here, it is assumed that Q and τ with the value less than 10^{-3} correspond to the entanglement measures disappearing. The value of Q vanishes outside of the regime surrounded by the solid line, and the value of τ vanishes outside of the regime surrounded by the dashed line).

4. Conclusions

In summary, three kinds of entanglement measures in the ground state of the $\{Cu_3\}$ single-molecular magnet with the applied magnetic field are calculated numerically based on the material parameters. These three kinds of measures characterize the pairwise entanglement, the 3-party entanglement and the total entanglement, respectively. The characteristics of entanglement with the applied magnetic field parallel to the plane of the $\{Cu_3\}$-type triangular spin ring are essentially different from the case of an applied magnetic field perpendicular to the plane. When the magnetic field is perpendicular to the plane, the values of pairwise entanglement and total entanglement measure have approximate plateaus within a low field range, while the 3-party entanglement vanishes. However, in the case of a magnetic field parallel to the plane all the measures undergo a sudden change at zero field. Moreover, different from the case of the magnetic field perpendicular to the plane, the in-plane magnetic field can induce the 3-party entanglement. Finally, the phase diagram of global entanglement characterized by the critical magnetic fields is presented.

References

[1] Karlsson A and Bourennane M 1998 *Phys. Rev. A* **58** 4394
[2] Hao J C, Li C F and Guo G C 2001 *Phys. Rev. A* **63** 054301
[3] Bruß D, DiVincenzo D P, Ekert A, Fuchs C A, Macchiavello C and Smolin J A 1998 *Phys. Rev. A* **57** 2368
[4] Amico L, Fazio R, Osterloh A and Vedral V 2008 *Rev. Mod. Phys.* **80** 517
[5] Bennett C H, Popescu S, Rohrlich D, Smolin J A and Thapliyal A V 2000 *Phys. Rev. A* **63** 012307
[6] Coffman V, Kundu J and Wootters W K 2000 *Phys. Rev. A* **61** 052306
[7] Meyer D A and Wallach N R 2002 *J. Math. Phys.* **43** 4273
[8] Brennen G K 2003 *Quantum Inf. Comput.* **3** 619
[9] Rungta P, Bužek V, Caves C M, Hillery M and Milburn G J 2001 *Phys. Rev. A* **64** 042315
[10] Hide J, Nakata Y and Murao M 2012 *Phys. Rev. A* **85** 042303
[11] Yu C S and Song H S 2006 *Phys. Rev. A* **73** 022325
[12] Montakhab A and Asadian A 2010 *Phys. Rev. A* **82** 062313

[13] Wang Y F, Cao J P and Wang Y P 2005 *Chin. Phys. Lett.* **22** 2151
[14] Wu K D, Zhou B and Cao W Q 2007 *Phys. Lett. A* **362** 381
[15] Chen S R, Xia Y J and Man Z X 2010 *Chin. Phys. B* **19** 050304
[16] Ren J Z, Shao X Q, Zhang S and Yeon K H 2010 *Chin. Phys. B* **19** 100307
[17] Pan H Z and Kuang L M 2004 *Chin. Phys. Lett.* **21** 424
[18] Xi X Q, Hao S R, Chen W X and Yue R H 2002 *Chin. Phys. Lett.* **19** 1044
[19] Zhang Y L and Zhou B 2011 *Acta Phys. Sin.* **60** 120301 (in Chinese)
[20] Thomas L, Lionti F, Ballou R, Gatteschi D, Sessoli R and Barbara B 1996 *Nature* **383** 145
[21] Wernsdorfer W and Sessoli R 1999 *Science* **284** 133
[22] Kortz U, Nellutla S, Stowe A C, Dalal N S, Rauwald U, Danquah W and Ravot D 2004 *Inorg. Chem.* **43** 2308
[23] Choi K Y, Matsuda Y H, Nojiri H, Kortz U, Hussain F, Stowe A C, Ramsey C and Dalal N S 2006 *Phys. Rev. Lett.* **96** 107202
[24] Stowe A C, Nellutla S, Dalal N S and Kortz U 2004 *Eur. J. Inorg. Chem.* **2004** 3792
[25] Choi K Y, Dalal N S, Reyes A P, Kuhns P L, Matsuda Y H, Nojiri H, Mal S S and Kortz U 2008 *Phys. Rev. B* **77** 024406
[26] Islam M F, Nossa J F, Canali C M and Pederson M 2010 *Phys. Rev. B* **82** 155446
[27] Bogani L and Wernsdorfer W 2008 *Nat. Mater.* **7** 179
[28] Leuenberger M N and Loss D 2001 *Nature* **410** 789
[29] Zhou B, Tao R B, Shen S Q and Liang J Q 2002 *Phys. Rev. A* **66** 010301
[30] Meier F, Levy J and Loss D 2003 *Phys. Rev. B* **68** 134417
[31] Troiani F, Ghirri A, Affronte M, Carretta S, Santini P, Amoretti G, Piligkos S, Timco G and Winpenny R E P 2005 *Phys. Rev. Lett.* **94** 207208
[32] Lehmann J, Gaita-Ariño A, Coronado E and Loss D 2007 *Nat. Nanotech.* **2** 312
[33] Kortz U, Al-Kassem N K, Savelieff M G, Al Kadi N A and Sadakane M 2001 *Inorg. Chem.* **40** 4742
[34] Trif M, Troiani F, Stepanenko D and Loss D 2008 *Phys. Rev. Lett.* **101** 217201
[35] Hou J M, Du L, Ding J Y and Zhang W X 2010 *Chin. Phys. B* **19** 110313
[36] Li J Q, Chen Z and Zhou B 2013 *Acta Phys. Sin.* **62** 190302 (in Chinese)
[37] Hill S and Wootters W K 1997 *Phys. Rev. Lett.* **78** 5022
[38] Wootters W K 1998 *Phys. Rev. Lett.* **80** 2245
[39] Endrejat J and Büttner H 2005 *Phys. Rev. A* **71** 012305